12th International Symposium on Turbulence and Shear Flow Phenomena (TSFP12)
Osaka, Japan (Online), July 19-22, 2022

HOMOCLINIC BIFURCATION, EDGE STATES, AND BOUNDARY CRISIS IN PLANE COUETTE FLOW

Julius Rhoan T. Lustro
Department of Mechanical Engineering
University of the Philippines Diliman
Magsaysay Avenue, Diliman, Quezon City,
Metro Manila 1101, Philippines
jtlustro@up.edu.ph

Yudai Shimizu
Measurement Instrumentation and Digital
Development Innovation Division
Toyota Motor Corporation
1, Toyota-cho, Toyota, Aichi 471-8571, Japan
yudai19891023@gmail.com

Genta Kawahara
Graduate School of Engineering Science
Osaka University,
1-3 Machikaneyama, Toyonaka, Osaka 560-8531, Japan
kawahara@me.es.osaka-u.ac.jp

ABSTRACT

We describe a rich bifurcation scenario that is related to the Nagata steady solution and time-periodic solutions in a plane Couette flow with streamwise period slightly longer than the minimal unit. We identify the presence of three homoclinic bifurcations that are linked with the creation (or destruction) of the time-periodic solutions. These periodic orbits function as homoclinic orbit to the lower-branch Nagata steady solution during homoclinic bifurcation at critical values of Reynolds number. In this computational domain, the lower branch of the Nagata steady solution acts as edge state at lower Reynolds number. At higher Reynolds number, the edge state switches from the lower-branch Nagata steady solution to the vigorous time-periodic solution during the creation of this limit cycle due to the homoclinic bifurcation. As a consequence, the stable manifold that forms the boundary which separates the basins of attraction of the laminar attractor and the time-periodic/chaotic attractor also switches respectively. Thus, the invariant solution that can trigger the transition to turbulence follows accordingly this switching of the edge state.

INTRODUCTION

Dynamical systems theory has been an invaluable tool in the last two decades in providing a theoretical explanation on the problem of transition to turbulence happening in wall-bounded shear flows (Eckhardt et al., 2007; Eckhardt et al., 2008; Kawahara et al., 2012). Transition in shear flows belongs to the subcritical category, where it has been found in numerical and experimental studies that crossing a threshold of a finite-amplitude disturbance can promote the transition process at Reynolds number below its critical value of linear instability. Under dynamical systems theory, the flow under subcritical transition category is considered as a system being regulated by invariant sets in phase space. In this context for shear flows, a stable invariant set which corresponds to the laminar flow coexists with a stable or marginally unstable invariant set which corresponds to the chaotic motion (turbulence) in the transitional regime. In the middle of these two sets exists an invariant set which forms the boundary that separates the basins of attraction between the laminar set and the chaotic set. This particular set is a saddle-type, which can either be an equilibrium or a time-periodic, and is often referred to as *edge state* (Skufca et al., 2006; Schneider et al., 2008; Vollmer et al., 2009). The edge state has a profound property that its stable manifold, which includes the edge state itself, forms, at least locally, the laminar-turbulent boundary. The initial conditions originating within this laminar-turbulent boundary will have trajectories that neither decay to the laminar nor become turbulent, but will be dynamically attracted to the edge state. For a simple edge state which has only one unstable direction, applying a strong enough perturbation results to a trajectory outside this boundary. As such, edge state can become a mechanism for controlling the flow (Kawahara, 2005).

In this paper we describe homoclinic bifurcation that relates the Nagata steady solution and the time-periodic solutions in a plane Couette flow with slightly longer streamwise period than the minimal unit by Kawahara and Kida (2001). An earlier study by Ehrenstein and Koch (1995) showed homoclinic bifurcation occurring in Blasius boundary-layer flow. They mentioned that the homoclinic orbits (Guckenheimer and Holmes, 1983; Palis and Takens, 1993; Ott, 2002) that are formed during homoclinic bifurcation are often related to intermittent physical bursting, which is also what van Veen and Kawahara (2011) suggested about the homoclinic orbits to a time-periodic edge state which they discovered in minimal plane Couette flow. The Blasius boundary-layer flow utilizes the Navier-Stokes equation which is simplified within the boundary layer. In contrast, we utilize the full Navier-Stokes equation in this study. In the next sections we discuss the flow configuration and computational schemes, then followed by the bifurcation diagram and their dynamical relevance.

FLOW CONFIGURATION & NUMERICAL METHODS

We study plane Couette flow which is considered as flow of Newtonian fluid between two parallel plates moving at a constant speed U. The plates are at a $2h$ distance apart and have a no-slip and impermeable surface. The streamwise, wall-normal, and spanwise coordinates are given as the $x-$, $y-$, and $z-$ directions, respectively, with their origin on the midplane. The Reynolds number is defined as $Re = Uh/\nu$, where ν is the kinematic viscosity of the fluid. Spatial periodicity is imposed on the flow in both the $x-$ and $z-$ directions. The streamwise period is given as $L_x = 1.93\pi h$ while the spanwise period is given as $L_z = 1.2\pi h$.

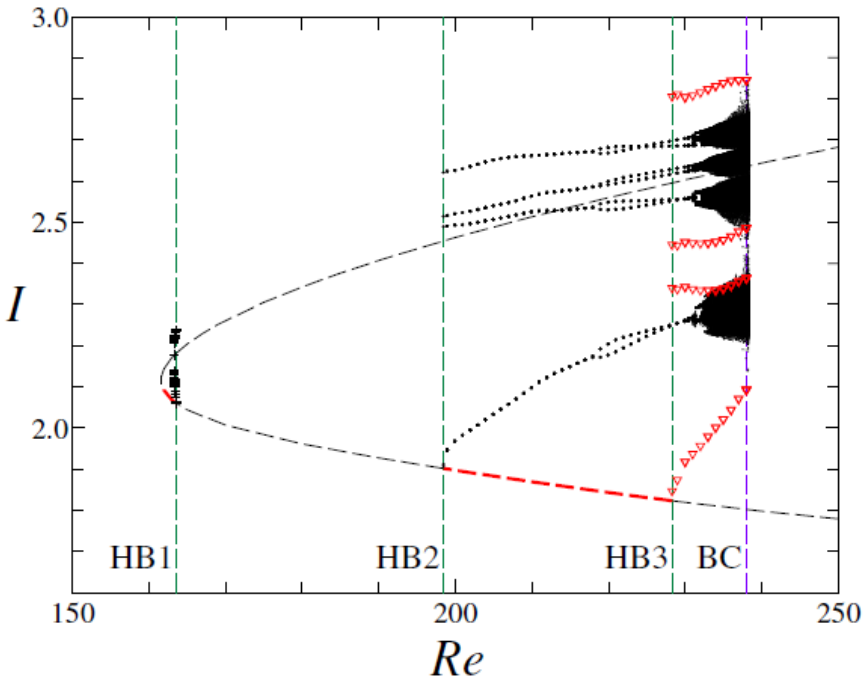

Figure 1. The bifurcation diagram of the Nagata steady solution in a plane Couette flow with slightly longer streamwise period than the minimal unit displayed as the value of the normalized input energy rate I as a function of the Re. Edge states are colored red.

We solve the incompressible Navier-Stokes equation using a spectral method. The numerical scheme is Crank-Nicolson method for the viscous terms and Adams-Bashforth method for the nonlinear terms, which is similar to the one used by Kim et al. (1987). Chebyshev-polynomial expansion is applied in the $y-$direction, while dealiased Fourier expansions are employed in both the $x-$ and $z-$directions. The numerically solved time-periodic solutions are contained in a subspace that is invariant under two spatial symmetries: (a) reflection in the streamwise and spanwise directions followed by a spanwise shift of $L_z/2$, and (b) reflection in the midplane followed by a streamwise shift of $L_x/2$. Numerical computations are carried on a resolution of $16 \times 33 \times 16$ in the $x-$, $y-$, and $z-$directions, respectively. Newton-GMRES (generalized minimal residual) method is used to compute for both the Nagata steady solution and time-periodic solutions, and Arnoldi iteration is used to examine the stability of the solutions to infinitesimal disturbance. These numerical procedures which use the time-stepping scheme mentioned above are essentially the same as what Sánchez et al. (2004) and Viswanath (2007) used. Edge-tracking method (Itano and Toh, 2001; Skufca et al., 2006; Schneider et al., 2008) is applied to search for a suitable initial condition to feed into the Newton-GMRES solver.

The trajectory of an initial point is determined by computing the normalized input and dissipation energy rates per unit time given respectively as

$$I = \frac{1}{2L_x L_z/h} \int_0^{L_x} \int_0^{L_z} \left(\left.\frac{\partial u}{\partial y}\right|_{y=-h} + \left.\frac{\partial u}{\partial y}\right|_{y=+h} \right) dxdz \qquad (1)$$

$$D = \frac{1}{2L_x L_z U^2/h} \int_0^{L_x} \int_{-h}^{+h} \int_0^{L_z} |\boldsymbol{\omega}|^2 \, dxdydz \qquad (2)$$

where u is the streamwise component of the velocity and $\boldsymbol{\omega}$ is the vorticity vector.

BIFURCATION SCENARIO TOWARDS TRANSITION TO TURBULENCE

Figure 1 shows the bifurcation diagram of the Nagata steady solution in the plane Couette flow in this study. The Nagata steady solution originates from a saddle-node bifurcation at $Re \approx 161.70$. The dashed lines denote unstable solution, while solid lines denote stable solution. The three time-periodic solutions **PO1**, **PO2**, and **PO3** are plotted using their maxima and minima values of I in one period and are represented by crosses, dots, and inverted open triangles, respectively. The location of the three homoclinic bifurcations **HB1**, **HB2**, and **HB3** are shown by the green vertical dashed lines. The lower branch of the Nagata steady solution is unstable and has only one real unstable eigenvalue, while the upper branch is initially stable. Inspection of the eigenvalues reveals that at $Re \approx 163.36$ the upper branch becomes unstable, i.e., a Hopf bifurcation occurs. A time-periodic solution (black crosses in Figure 1) arises from the upper branch of the Nagata steady solution due to the Hopf bifurcation. This periodic orbit **PO1** disappears due to the occurrence of homoclinic bifurcation **HB1** at $Re_{HB1} \approx 163.58$.

A new homoclinic bifurcation **HB2** occurs at $Re_{HB2} \approx 198.50$ and another time-periodic solution (black dots in Figure 1) appears. This periodic orbit **PO2** is initially stable and it encounters an instability at $Re \approx 219.00$ and a period-doubling cascade begins. The period-doubling cascade results to a chaotic attractor, which encounters a boundary crisis **BC** at $Re_{BC} \approx 238.01$. The boundary crisis **BC** at $Re_{BC} \approx 238.01$ is manifested by the contact of the chaotic attractor **CA** with another time-periodic solution (red inverted open triangles in Figure 1). This vigorous periodic orbit **PO3**, which comes in contact with **CA**

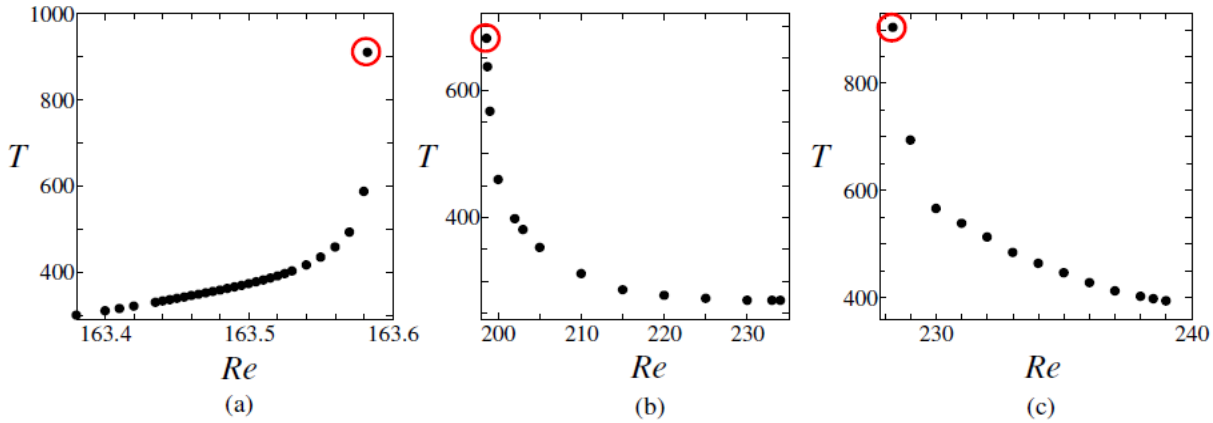

Figure 2. Variation of period T of the three time-periodic solutions with respect to Re for (a) **PO1**, (b) **PO2**, and (c) **PO3**.

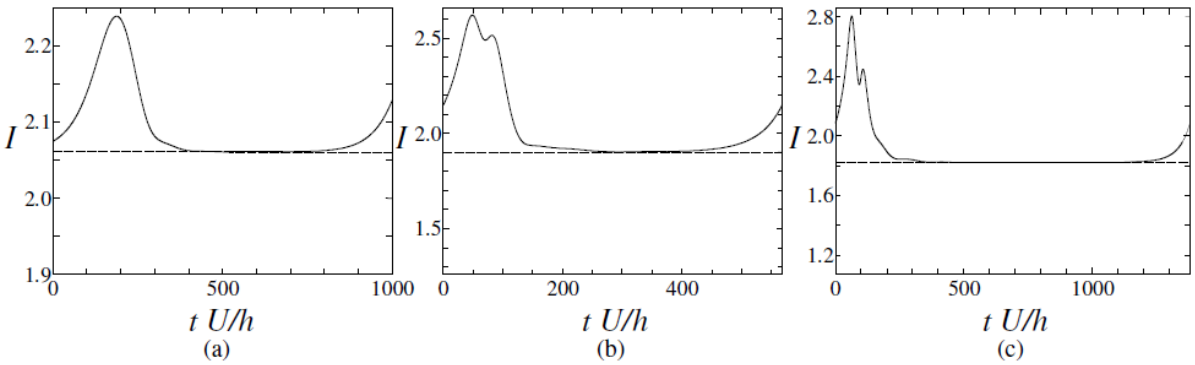

Figure 3. Approach of the trajectory of (a) **PO1**, (b) **PO2**, and (c) **PO3** to the trajectory of the lower-branch Nagata steady solution at Re of the encircled points in Figure 2.

during **BC**, appears from a homoclinic bifurcation **HB3** at $Re_{HB3} \approx 228.32$. The critical Reynolds number for **BC** is shown by the purple vertical dashed line in Figure 1. This period-doubling cascade that leads to a chaotic attractor and subsequent boundary crisis with a time-periodic solution (which is an edge state) is reminiscent of similar bifurcation scenario in plane Couette flow of different computational domains.

HOMOCLINIC BIFURCATION, EDGE STATES, & BOUNDARY CRISIS

A time-periodic solution, which is a limit cycle, appears or disappears at the Re where the homoclinic bifurcation occurs. The periodic orbit appearing during homoclinic bifurcation constitutes the homoclinic orbit to the lower-branch Nagata steady solution. Near the homoclinic bifurcation the trajectory of the periodic orbit that approaches the lower-branch Nagata steady solution is extended and goes to infinity as the Re for homoclinic bifurcation is being approached asymptotically, as seen in Figure 2. This monotonic increase in the period T of the periodic orbits as the Re for homoclinic bifurcation is being approached is an example of a global bifurcation known as infinite-period bifurcation (Strogatz, 1994; Wiggins, 1998). In Figure 3, it is shown that this extension of the period T near the site of the homoclinic bifurcation is the part of the periodic orbit trajectory that spends more time during the approach to the lower-branch Nagata steady solution. Indeed, as shown in Figure 4, inspection of the flow structures of these extended parts of the periodic orbits at the Re encircled in Figure 2 shows striking resemblance with the flow structures of the lower-branch Nagata steady solution at the same Re. Figures on the left (a, c, and e) are on the extended portions of the trajectory of the periodic orbits **PO1**, **PO2**, and **PO3**, respectively, that are approaching the lower-branch Nagata steady solution. Figures on the right (b, d, and f) are on the lower-branch Nagata steady solution at Re corresponding to those of (a, c, and e), respectively. Gray corrugated isosurfaces of the null of streamwise velocity represent streaks. The red and blue isosurfaces of the second invariant of a velocity gradient tensor represent clockwise and counter-clockwise streamwise vortex tubes, respectively.

Figure 5 illustrates the occurrence of homoclinic bifurcation. The black dot is the lower-branch Nagata steady solution, which is a fixed point. The light blue and light green lines denote the unstable and stable manifolds to the fixed point (saddle-type), respectively. For $Re < Re_{HB2}$ homoclinic bifurcation just not occur yet and all trajectories from the fixed point goes to the laminar attractor. For $Re = Re_{HB2}$, a homoclinic bifurcation occurs and **PO2**, a limit cycle, appears. This limit cycle grows in size as Re_{HB2} is being approached, yielding an orbit of infinite period. This infinite-period orbit actually serves as homoclinic orbit to the fixed point. For $Re > Re_{HB2}$, all trajectories from the fixed point are eventually attracted to the limit cycle **PO2** that is denoted by the dark blue curve. Depending on the direction of the appearance of the periodic orbit, either above or below the Re where the homoclinic bifurcation occurs, the trajectories are attracted either to the laminar attractor or to the other attractor

which is the limit cycle that appears. As such as seen in the bifurcation diagram in Figure 1, the occurrences of homoclinic bifurcations are associated with the existence of edge state. The edge states are indicated with red color in Figure 1. At lower Re, the lower-branch Nagata steady solution serves as the edge state between the laminar attractor and the other attractor, which is the limit cycle. This means that at lower values of Re the steady edge state and its stable manifold forms the boundary that separates the basins of attraction between the laminar attractor and the limit cycle attractor. For $163.36 < Re < 163.58$, the steady edge state and its stable manifold forms the basin boundary between the laminar attractor and **PO1**. For $198.50 < Re < 228.32$, the steady edge state and its stable manifold forms the basin boundary between the laminar attractor and **PO2** and its subsequent period-doubling branch. Unfortunately, we did not find any limit cycle or bifurcation event for $163.58 < Re < 198.50$, and so no edge state exists in that range of Re.

At higher Re, we observe a switching of edge states. This switching of edge states happens during homoclinic bifurcation **HB3** at $Re_{HB3} \approx 228.32$, where the edge state is changed from the lower-branch Nagata steady solution to the newly created limit cycle **PO3** due to **HB3**. In addition to the creation of the vigorous time-periodic solution **PO3** during **HB3**, **HB3** also serves as a mechanism that triggers the switching of edge states. For $228.32 < Re < 238.01$, this vigorous periodic orbit **PO3**, which is unstable, becomes the edge state between the laminar attractor and the period-doubling branch of **PO2** that turns subsequently into the chaotic attractor **CA**. As a consequence, aside from the edge state switching, the formation of the boundary that separates the basins of attraction between the laminar attractor and the period-doubling branch of **PO2**/chaotic attractor **CA** also switches from the steady edge state to this vigorous time-periodic edge state **PO3** (together with their respective stable manifolds) during **HB3**.

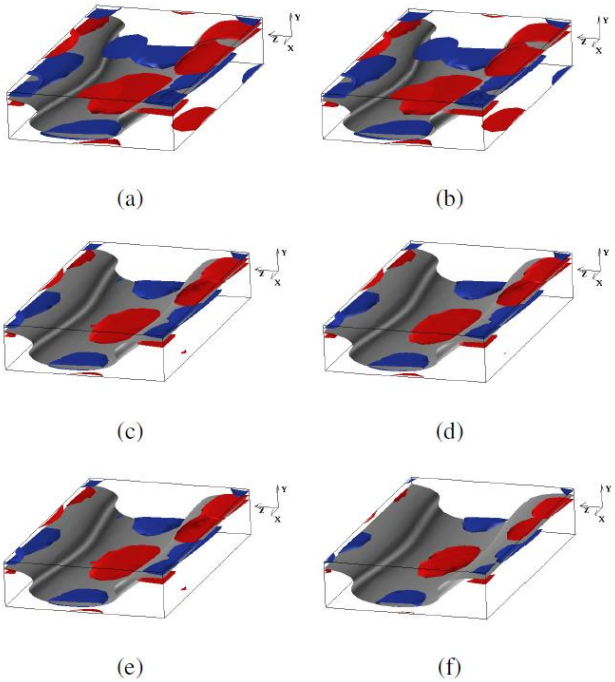

Figure 4. Visualization of the flow structures of the extended portions of the trajectory of the periodic orbits (on the left) and the lower-branch Nagata steady solution (on the right) very near **HB1**, **HB2**, and **HB3**, from top to bottom respectively.

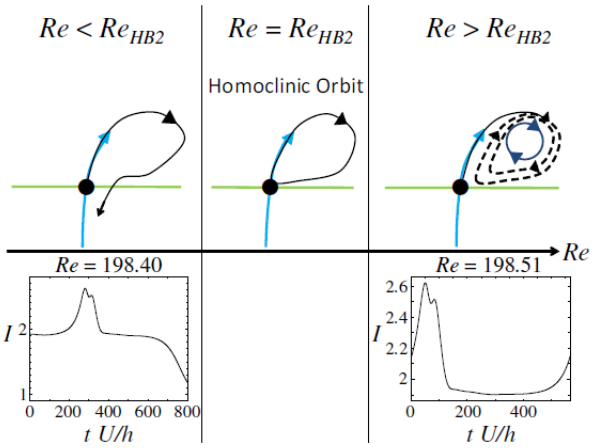

Figure 5. Sketch of the appearance of homoclinic bifurcation **HB2** for increasing Re in the vicinity of $Re_{HB2} \approx 198.50$.

In Figure 1 we see that during boundary crisis **BC** at $Re_{BC} \approx 238.01$ all of the four red inverted open triangles which represent the maxima and minima values of **PO3** fall onto the black dots which represent **CA**. **PO3** is mentioned as a vigorous time-periodic solution earlier because its I and D energy values sometimes exhibit that of turbulent behavior. Figure 6 shows that the trajectory of the chaotic attractor **CA** comes nearer to the time-periodic edge state **PO3** in the vicinity of the Re of the boundary crisis **BC**, where **CA** comes in contact with **PO3** at $Re_{BC} \approx 238.01$. The approach is more evident as the distance between the minima of **CA** and **PO3** shrinks for increasing Re towards its critical value (see the bottom part of Figure 6a and Figure 6b). This shrinking distance is measured quantitatively by computing d between the minima of **CA** and **PO3** as shown in Figure 6 using the quantities below.

$$d_I = \frac{\sqrt{\int_0^T [I_{CA}(t+\tau) - I_{PO3}(t)]^2 dt}}{\int_0^T [I_{CA}(t)]^2 dt} \tag{3}$$

$$d_D = \frac{\sqrt{\int_0^T [D_{CA}(t+\tau) - D_{PO3}(t)]^2 dt}}{\int_0^T [D_{CA}(t)]^2 dt} \tag{4}$$

The subscripts **CA** and **PO3** correspond to the chaotic attractor and time-periodic edge state, respectively, while t denotes the time period shift that is optimised so that d_I and d_D may be minimal at each Re. Figure 7 shows that both d_I (red circles) and d_D (blue circles) becomes smaller and smaller as the value of the critical Re of boundary crisis is being approached. These values of d_I and d_D are at the minimum, i.e., closest to zero, when the boundary crisis happens at Re_{BC}. We note that this approach is only a partial and not a full one because of the inherent instability of the **CA** and the unstable characteristics of **PO3**. We confirm that there is a time dependence of this approach to the local minima of **PO3** and that the threshold time is short in comparison with the period of **PO3**. Nevertheless, the numerical approach achieved here is sufficient to give evidence for the real approach of **CA** to **PO3**.

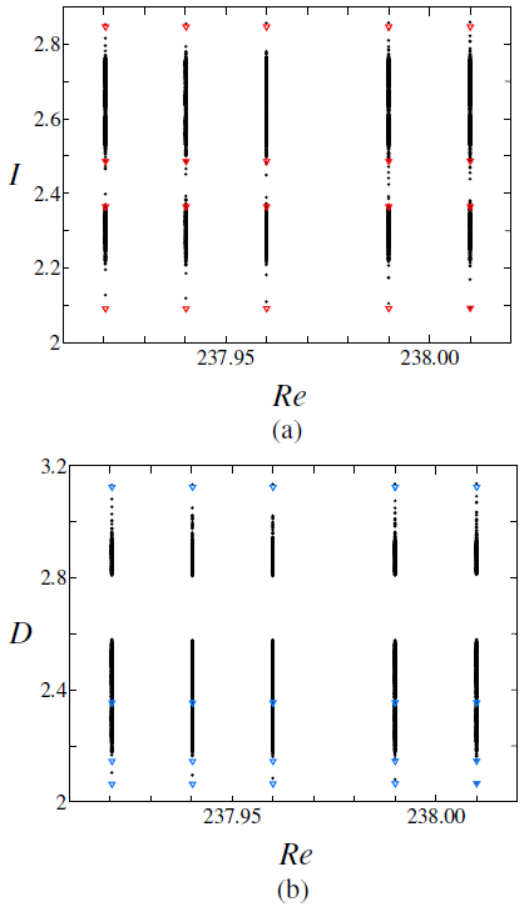

Figure 6. Approach of the chaotic attractor **CA** to the time-periodic edge state **PO3** during the boundary crisis **BC**.

Transient turbulence which eventually relaminarises is seen for Re above $Re_{BC} \approx 238.01$. Such appearance of transient chaotic behavior is associated with the occurrence of boundary crisis in chaotic dynamical systems (Ott, 2002; Lai and Tel, 2011). For other plane Couette flow systems, such transient turbulence that eventually relaminarizes was also observed after the occurrence of boundary crisis, such as in Kreilos and Eckhardt (2012), Shimizu et al. (2014), and Lustro et al. (2019). In both of our works in the minimal plane Coutte flow previously (Lustro et al., 2019) and in a slightly longer plane Couette flow in this study, the boundary crisis is found to be associated with the approach of the chaotic attractor with a time-periodic edge state.

The switching of edge states as well as the invariant sets which form the boundary that separates the basins of attraction between the laminar attractor and the time-periodic/chaotic attractor in this study are novel observations on transitional shear flows. To our knowledge, these observations are also new findings for other chaotic dynamical systems. Both of these switching events happen due to the presence of homoclinic bifurcation at a critical value of Re ($Re_{HB3} \approx 228.32$). For transitional plane Couette flow, it was reported that the structure of the basin boundary between the laminar attractor and the chaotic set is fractal. Such fractal basin boundary, which is also known as *edge of chaos* (Skufca et al., 2006), is due to the bifurcation from a simple, smooth basin boundary. The same relationship between this fractal basin boundary and chaotic saddle formation has also been reported in transitional plane

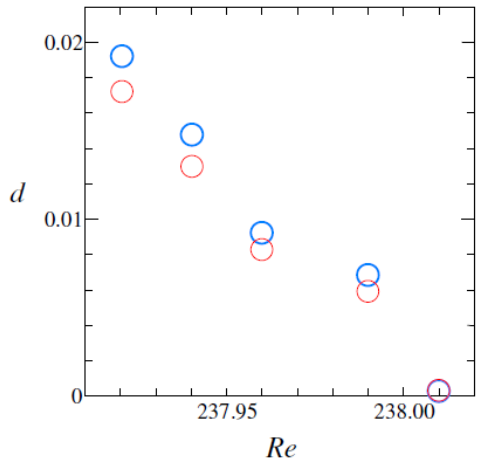

Figure 7. A quantitative measure of the approach of the chaotic attractor **CA** to the time-periodic edge state **PO3** during the boundary crisis **BC**.

Couette flow (Skufca et al., 2006; Kreilos and Eckhardt, 2012; Shimizu et al., 2014; Lustro et al., 2019).

Homoclinic bifurcation is a global bifurcation which occurs when a periodic orbit touches the lower-branch Nagata steady solution, which is a fixed point. At the homoclinic bifurcation point, the periodic orbit takes the role of homoclinic orbit to this fixed point. Therefore, this homoclinic orbit to the fixed point is not associated to chaotic dynamics, but rather to a limit cycle, i.e., the periodic orbit. This lack of chaotic dynamics is due to the absence of the transversal intersection of the stable and unstable manifolds, i.e., homoclinic orbits, to the fixed point. A Shilnikov criteria, i.e., finding a homoclinic orbit that is transversal to a plane containing the fixed point must be imposed in order to obtain this transversal intersection of the stable and unstable manifolds (Guckenheimer and Holmes. 1983; Wiggins, 1988; Shilnikov, 1970)

In our recent work in minimal plane Couette flow (Lustro et al., 2019), we showed that the onset of transient turbulence that eventually relaminarizes happens due to boundary crisis. Such boundary crisis is generated by the tangency of homoclinic orbits to a time-periodic edge state. Hence, the tangency of homoclinic orbits to a time-periodic edge state provides the mechanism for the onset of transient turbulence in minimal plane Couette flow. This is because of the presence of Smale horseshoe in transversal homoclinic orbits following the Smale-Birkhoff theorem in chaotic dynamical systems (Guckenheimer and Holmes, 1983; Palis and Takens, 1993; Strogatz, 1994; Ott, 2002). This transient turbulent behavior that is observed in this study after the boundary crisis **BC** may perhaps also be associated with homoclinic orbits to the time-periodic edge state **PO3**, if they exist. The finding of such homoclinic obits to **PO3** is left for future work.

CONCLUSION

We reported homoclinic bifurcations in plane Couette flow with slightly longer streamwise period than the minimal unit. Three homoclinic bifurcations are shown to be related to the appearance or disappearance of their corresponding time-periodic solutions. At Re where the homoclinic bifurcations occur, the corresponding periodic orbits function as homoclinic orbits to the lower-branch Nagata steady solution. The most

energetic of these periodic orbits, which we called the vigorous periodic orbit **PO3**, serves as the edge state between the laminar attractor and time-periodic/chaotic attractor at higher values of Re. At lower values of Re the lower-branch Nagata steady solution serves as the edge state between the laminar attractor and time-periodic attractor (limit cycle). The switching of edge states from the lower-branch Nagata steady to the vigorous periodic orbit **PO3** occurs due to the creation of **PO3** during homoclinic bifurcation **HB3**.

The periodic orbit **PO2** is initially stable but encounters an instability which leads to a period-doubling cascade that later becomes a chaotic attractor **CA**. A boundary crisis happens when the chaotic attractor **CA** touches the periodic edge state **PO3** at $Re_{BC} \approx$ 238.01. For $Re >$ 238.01, transient turbulence which eventually relaminarizes is observed consistently with the previous result for the minimal unit. This boundary crisis has been confirmed qualitatively and quantitatively.

The rich bifurcation scenario presented here for a fluid flow system with two kinds of edge states adds to the repertoire of dynamical systems approach to understanding the subcritical transition to turbulence in shear flows. Finally, the discovery of homoclinic bifurcation here is meaningful for bifurcation theory as it provides evidence of such event in a system governed by the full Navier-Stokes equation.

REFERENCES

Eckhardt, B., Schneider, T. M., Hof, B., and Westerweel, J., 2007, "Turbulence transition in pipe flow", *Annu. Rev. Fluid Mech.* 39, pp. 447–468.

Eckhardt, B., Faisst, H., Schmiegel, A., and Schneider, T. M., 2008, "Dynamical systems and the transition to turbulence in linearly stable shear flows", *Phil. Trans. R. Soc. Lond. A* 366, pp. 1297–1315.

Ehrenstein, U., and Koch, W., 1995, "Homoclinic bifurcation in Blasius boundary-layer flow", *Phys. Fluids* 7, pp. 1282.

Graham, M. D., and Floryan, D., 2021, "Exact coherent states and the nonlinear dynamics of wall-bounded turbulent flows", *Annu. Rev. Fluid Mech*. 53, pp. 227–253.

Guckenheimer, J., and Holmes, P., 1983, *Nonlinear Oscillations, Dynamical Systems, and Bifurcations of Vector Fields*, Springer-Verlag, New York.

Itano, T., and Toh, S., 2001, "The dynamics of bursting process in wall turbulence", *J. Phys. Soc. Jpn*. 70, pp. 703–716.

Kawahara, G., and Kida, S., 2001, "Periodic motion embedded in plane Couette turbulence: regeneration cycle and burst", *J. Fluid Mech*. 449, pp. 291–300.

Kawahara, G., 2005, "Laminarization of minimal plane Couette flow: Going beyond the basin of attraction of turbulence", *Phys. Fluids.* 17, pp. 041702.

Kawahara, G., Uhlmann, M., and van Veen, L., 2012, "The significance of simple invariant solutions in turbulent flows", *Annu. Rev. Fluid Mech*. 44, pp. 03–225.

Kim, J., Moin, P., and Moser, R. D., 1987, "Turbulence statistics in fully developed channel flow at low Reynolds number", *J. Fluid Mech*. 177, pp. 133–166.

Kreilos, T., and Eckhardt, B., 2012, "Periodic orbits near onset of chaos in plane Couette flow", *Chaos* 22, pp. 047505.

Lai, C., and Tel, T., 2011, *Transient Chaos*, Springer-Verlag, New York.

Lustro, J. R. T., Kawahara, G., van Veen, L., Shimizu, M., and Kokubu, H., 2019, "The onset of transient turbulence in minimal plane Couette flow", *J. Fluid Mech*. 862, pp. R2.

Ott, E., 2002, *Chaos in Dynamical Systems*, 2nd ed., Cambridge University Press, United Kingdom.

Palis, J., and Takens, F., 1993, *Hyperbolicity and Sensitive Chaotic Dynamics at Homoclinic Bifurcations*, Cambridge University Press, Great Britain.

Sánchez, J., Net, M., García-Archilla, B., and Simó, C., 2004, "Newton-Krylov continuation of periodic orbits for Navier-Stokes flows", *J. Comput. Phys.* 201, pp. 13–33.

Schneider, T. M., Gibson, J. F., Lagha, M., Lillo, F. D., and Eckhardt, B., 2008, "Laminar-turbulent boundary in plane Couette flow", *Phys. Rev. E.* 78, pp. 037301.

Shilnikov, L. P., 1970, "A contribution to the problem of the structure of an extended neighborhood of a rough equilibrium state of saddle-focus type", *Mat. Sb.* 81, pp. 92–103.

Shimizu, M., Kawahara, G., Lustro, J. R. T., and van Veen, L., 2014, "Route to chaos in minimal plane Couette flow", in *ECCOMAS Congress*, CIMNE, Barcelona.

Skufca, J. D., Yorke, J. A., and Eckhardt, B., 2006, "Edge of chaos in a parallel shear flow", *Phys. Rev. Lett*. 96, pp. 174101.

Strogatz, S. H., 1994, *Nonlinear Dynamics and Chaos: With Applications to Physics, Biology, Chemistry, and Engineering*, Perseus, Massachusetts.

Vollmer, J., Schneider, T. M., and Eckhardt, B., 2009, "Basin boundary, edge of chaos, and edge state in a two-dimensional model", *New J. Phys.* 11, pp. 013040.

van Veen, L., and Kawahara, G., 2011, "Homoclinic tangle on the edge of shear turbulence", *Phys. Rev. Lett.* 107, pp. 114501.

Viswanath, D., 2007, "Recurrent motions within plane Couette turbulence", *J. Fluid Mech*. 580, pp. 339–358.

Wiggins, S., 1988, *Global Bifurcations and Chaos: Analytical Methods*, Springer-Verlag, New York.